Supplementary Table 1: Plasmids and Parts

Addgene	Code	Origin	Regulator	Reporter	Marker
172542	pAVR4	p15A	$VanR^{AM}$	mRFP	Carbenicillin
172543	pCLxR4	ColA	LuxR	mRFP	Carbenicillin
172544	pDCyR4	CloDF13	$CymR^{AM}$	mRFP	Carbenicillin
172545	pELlR4	pBR322	LacI	mRFP	Carbenicillin
172546	pEVR4	pBR322	$VanR^{AM}$	mRFP	Carbenicillin
172547	pELxR4	pBR322	LuxR	mRFP	Carbenicillin
172548	pECyR4	pBR322	$CymR^{AM}$	mRFP	Carbenicillin
172549	pAVR2	p15A	$VanR^{AM}$	mRFP	Kanamycin
172550	pCLxR2	ColA	LuxR	mRFP	Kanamycin
172551	pCVR2	ColA	$VanR^{AM}$	mRFP	Kanamycin
172552	pCCyR2	ColA	$CymR^{AM}$	mRFP	Kanamycin
172553	pCLlR2	ColA	LacI	mRFP	Kanamycin
172554	pDCyR2	CloDF13	$CymR^{AM}$	mRFP	Kanamycin
172555	pELlR2	pBR322	LacI	mRFP	Kanamycin
172557	pCLxR6	ColA	LuxR	mRFP	Streptomycin
172558	pDCyR6	CloDF13	$CymR^{AM}$	mRFP	Streptomycin
172559	pDLlR6	CloDF13	LacI	mRFP	Streptomycin
172560	pDLxR6	CloDF13	LuxR	mRFP	Streptomycin
172562	pELlR6	pBR322	LacI	mRFP	Streptomycin
172563	pAVR1	p15A	$VanR^{AM}$	mRFP	Chloramphenicol
172564	pALxR1	p15A	LuxR	mRFP	Chloramphenicol
172565	pACyR1	p15A	$CymR^{AM}$	mRFP	Chloramphenicol
172566	pALlR1	p15A	LacI	mRFP	Chloramphenicol
172567	pCLxR1	ColA	LuxR	mRFP	Chloramphenicol
172568	pDCyR1	CloDF13	$CymR^{AM}$	mRFP	Chloramphenicol
172569	pELlR1	pBR322	LacI	mRFP	Chloramphenicol
172570	pELxG4	pBR322	LuxR	GFPmut3	Carbenicillin
172571	pEVG4	pBR322	$VanR^{AM}$	GFPmut3	Carbenicillin

Supplementary Table 2: Regulatory Element Sources

Part	Native Host	Regulator Source	Promoter Source
$CymR^{AM}/P_{CymRC}$	*Pseudomonas putida*	sAJM.1506 (1–3)	Synthetic (1, 3)
$LacI/P_{LlacO-1}$	*Escherichia coli*	pTacHis	iGEM
$LuxR/P_{LuxB}$	*Aliivibrio fischeri*	sAJM.1506 (3, 4)	Synthetic (3, 4)
$VanR^{AM}/P_{VanCC}$	*Caulobacter crescentus*	sAJM.1506 (3, 5, 6)	Synthetic (3, 6)

Supplementary Table 3: Inducers

Inducer	Source	Solvent	Stock	Standard concentration
Cumate	Sigma 268402	EtOH	100 mM	100 µM
IPTG	Sigma I6758	Water	1 M	100 µM
N-(3-oxohexanoyl) homoserine lactone (OC6)	Sigma K3007	DMF	10 mM	10 µM
Vanillate	Sigma V2250	EtOH	100 mM	100 µM

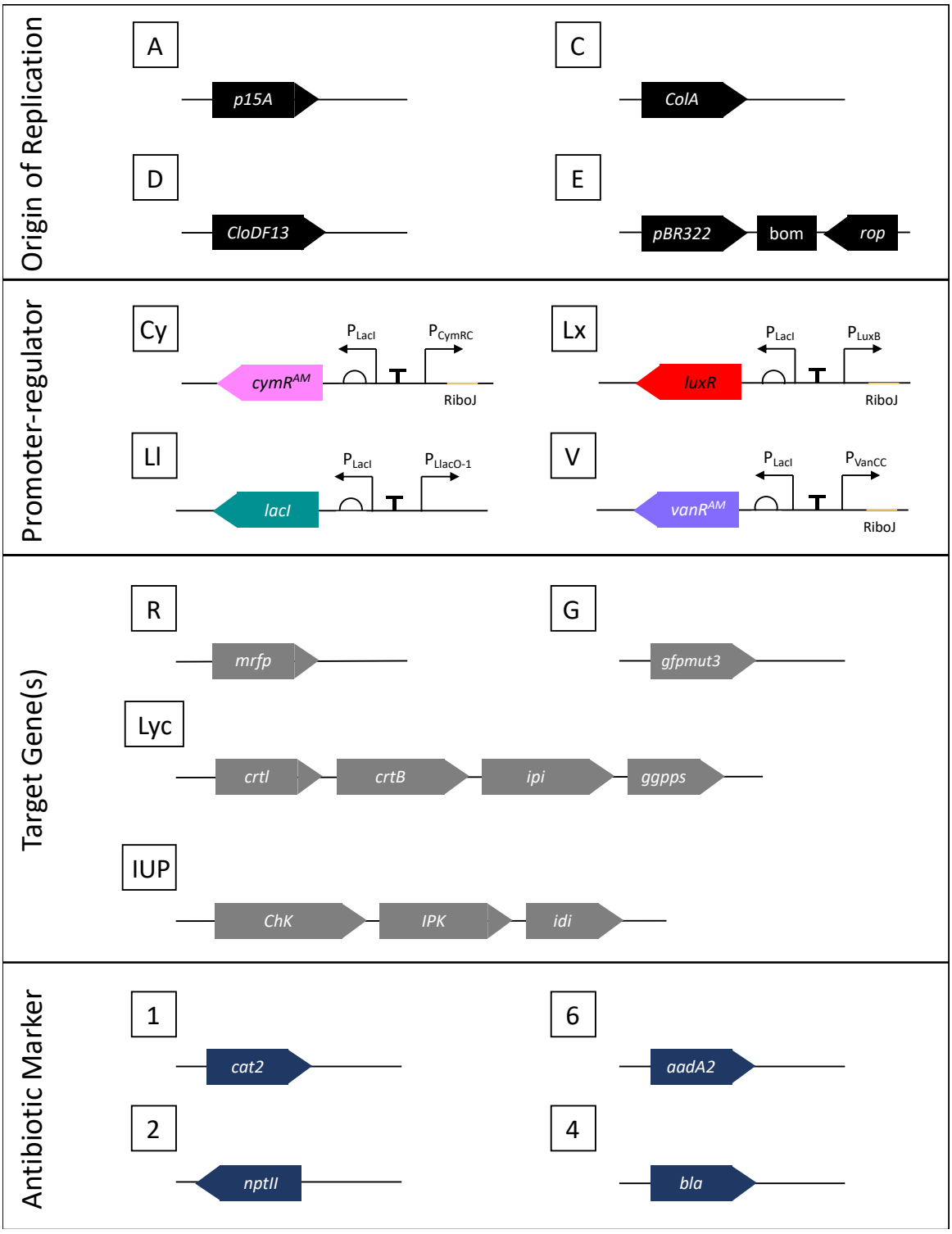

Supplementary Figure 1: Plasmid toolbox genetic parts included in study.
Origin parts: p15A (7), ColA (7), CloDF13 (7), and pBR322 (7). Promoter-regulator parts as described previously (8) and in Supplementary Table 1. Target gene(s) including mRFP (9), GFPmut3 (9), and operons of a previously described lycopene pathway (10). Marker parts including chloramphenicol resistance (11) (*cat2*), kanamycin resistance (11) (*nptII*), streptomycin resistance (7) (*aadA2*), and ampicillin resistance (11) (*bla*).

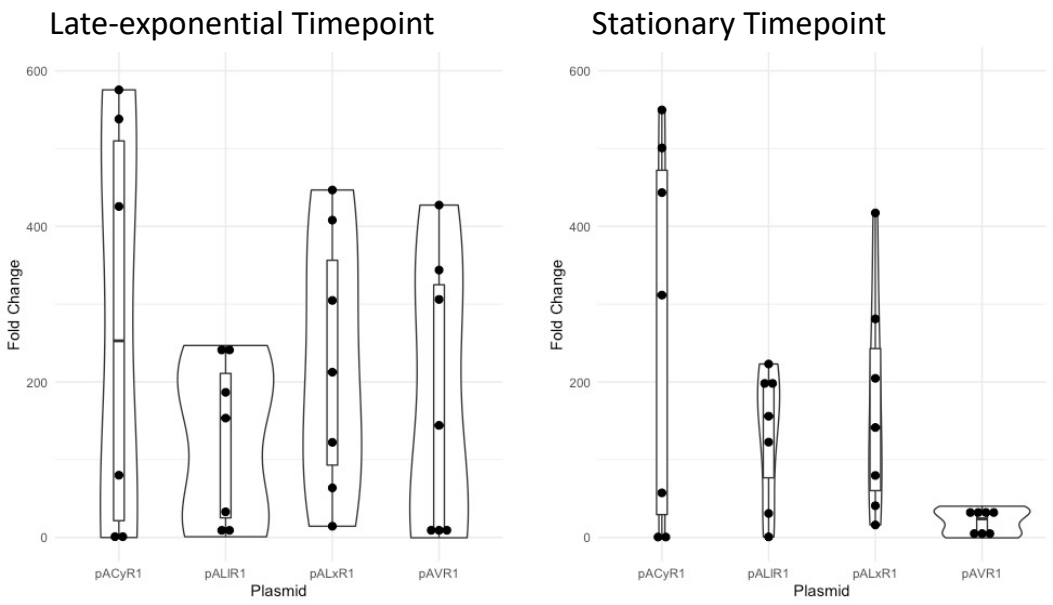

Supplementary Figure 2: Distribution of fold change across titrated inducer concentrations. Fold change data displayed as violin plots with inlaid boxplots to show distribution at two timepoints.

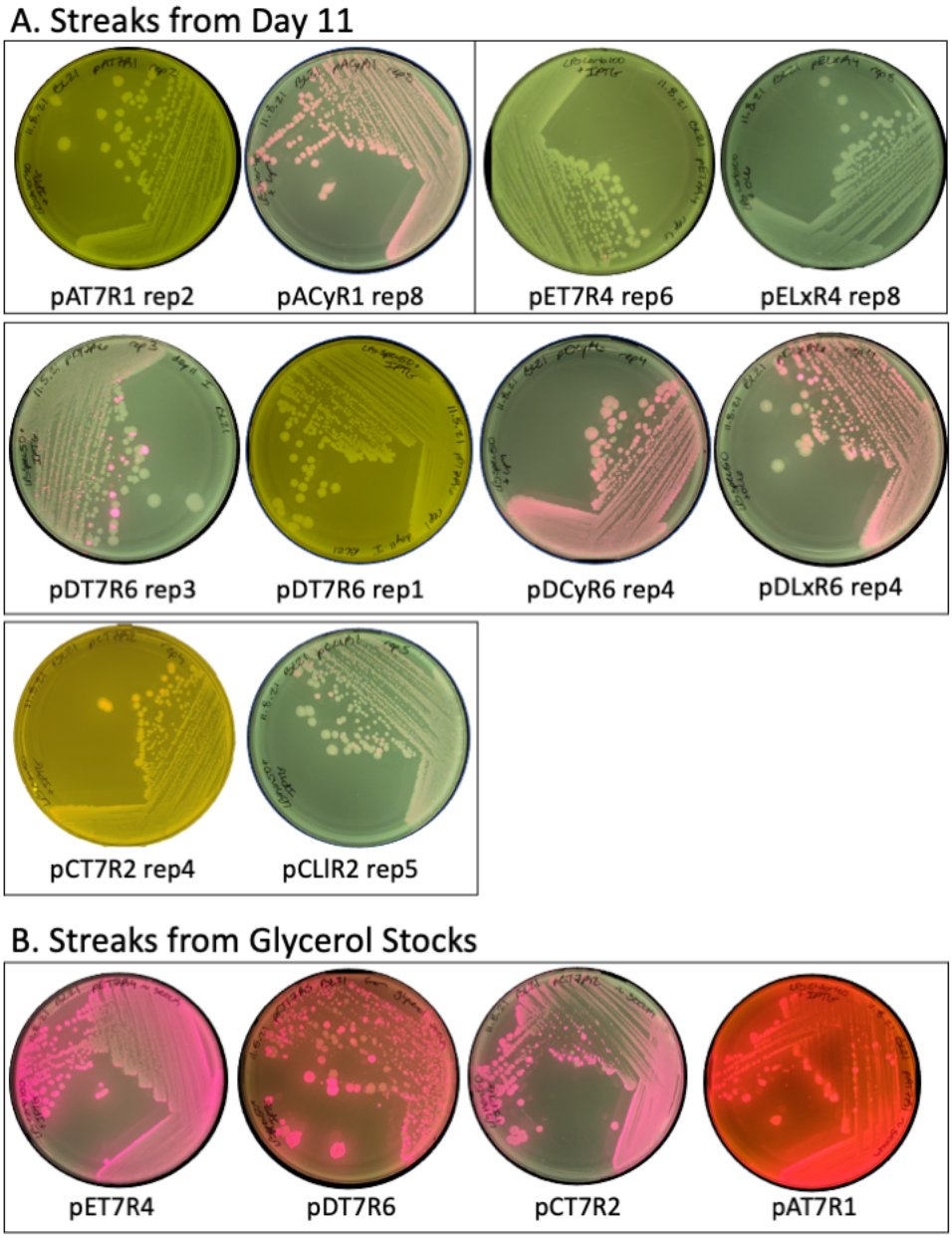

Supplementary Figure 3: Stability Screen Plate Images.
(A.) Agar plates with selection were spread with cognate inducer and *E. coli* BL21(DE3) strains from day 11 of the extended passage experiment were struck out and photographed under blue light to visualize colonies with red fluorescence. (B.) Glycerol stocks of strains freshly transformed with Duet plasmids were struck on to selection plates spread with cognate inducer.

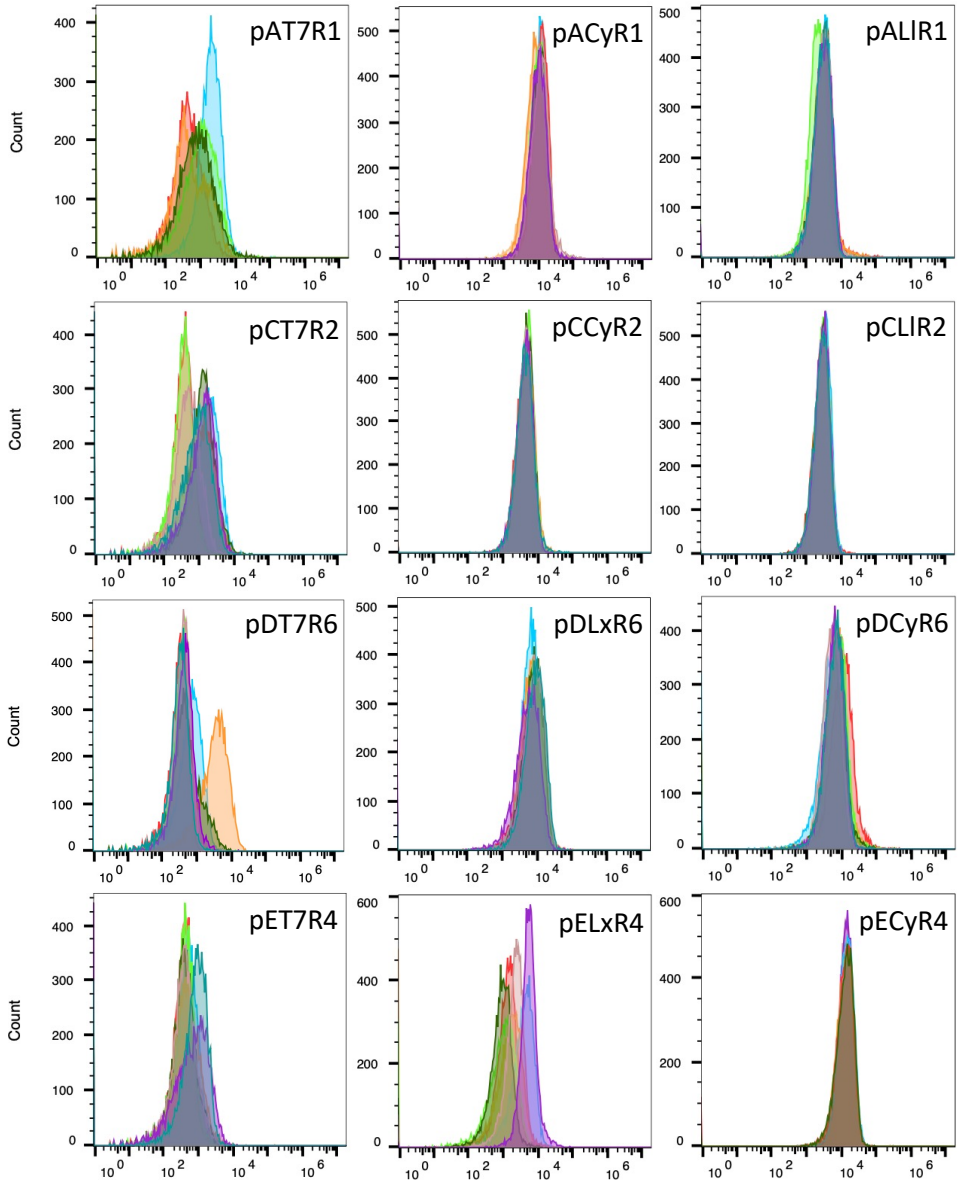

Supplementary Figure 4: Flow cytometry histograms.
Cultures from day 12 of the extended passage experiment were measured with flow cytometry and FlowJo v10 (TreeStar Inc.) was used to analyze the data. All replicates of each plasmid overlaid within each histogram with relative fluorescence displayed on the x-axis and cell count on the y-axis. Replicates with an OD < 0.2 excluded from dataset.

Sample Name	Geometric Mean	CV
pAT7R1.8	463	296
pAT7R1.7	574	390
pAT7R1.5	259	170
pAT7R1.4	1727	373
pAT7R1.3	254	357
pCT7R2.8	500	181
pCT7R2.7	646	113
pCT7R2.6	313	147
pCT7R2.5	1009	166
pCT7R2.4	228	457
pCT7R2.3	514	2217
pCT7R2.2	909	121
pCT7R2.1	251	1273
pDT7R6.8	234	173
pDT7R6.7	370	359
pDT7R6.6	339	137
pDT7R6.5	379	1002
pDT7R6.4	318	2329
pDT7R6.3	1476	95
pDT7R6.2	491	1049
pDT7R6.1	220	89
pET7R4.8	648	127
pET7R4.7	351	745
pET7R4.6	289	165
pET7R4.5	287	454
pET7R4.4	287	2700
pET7R4.3	314	2828
pET7R4.2	376	100
pET7R4.1	278	316

Sample Name	Geometric Mean	CV
pACyR1.8	8487	261
pACyR1.7	10862	708
pACyR1.6	8931	737
pACyR1.5	8857	112
pACyR1.4	6958	187
pACyR1.3	11156	113
pACyR1.2	10458	143
pACyR1.1	6215	151
pCCyR2.8	4182	509
pCCyR2.7	4081	53
pCCyR2.6	4130	54
pCCyR2.5	4237	140
pCCyR2.4	4551	107
pCCyR2.3	4580	73
pCCyR2.2	4331	59
pCCyR2.1	3863	59
pDLxR6.8	7762	135
pDLxR6.7	4172	96
pDLxR6.6	6954	137
pDLxR6.5	6550	65
pDLxR6.4	6412	66
pDLxR6.3	6090	238
pDLxR6.2	5847	71
pDLxR6.1	5756	67
pECyR4.7	12627	86
pECyR4.5	12349	68
pECyR4.4	11156	250
pECyR4.3	12436	114
pECyR4.2	10890	75
pECyR4.1	12035	91

Sample Name	Geometric Mean	CV
pALIR1.8	2853	97
pALIR1.7	2828	134
pALIR1.6	2969	279
pALIR1.5	2909	216
pALIR1.4	1934	199
pALIR1.3	2758	402
pALIR1.2	3134	91
pALIR1.1	3240	429
pCLIR2.8	2726	49
pCLIR2.7	2870	266
pCLIR2.6	2858	48
pCLIR2.5	2778	48
pCLIR2.4	2840	62
pCLIR2.3	2823	48
pCLIR2.2	3179	179
pCLIR2.1	2721	415
pDCyR6.8	5494	89
pDCyR6.7	5670	80
pDCyR6.6	4800	162
pDCyR6.5	5136	171
pDCyR6.4	6140	146
pDCyR6.3	5724	842
pDCyR6.2	3302	232
pDCyR6.1	7960	470
pELxR4.7	5456	150
pELxR4.6	1993	201
pELxR4.5	935	603
pELxR4.4	795	166
pELxR4.3	908	669
pELxR4.2	2117	117
pELxR4.1	1317	304

Supplementary Table 4: Flow cytometry statistics.
Statistical analysis for all replicates included in Supplementary Figure 4. Analysis competed using FlowJo v10 (TreeStar Inc.).

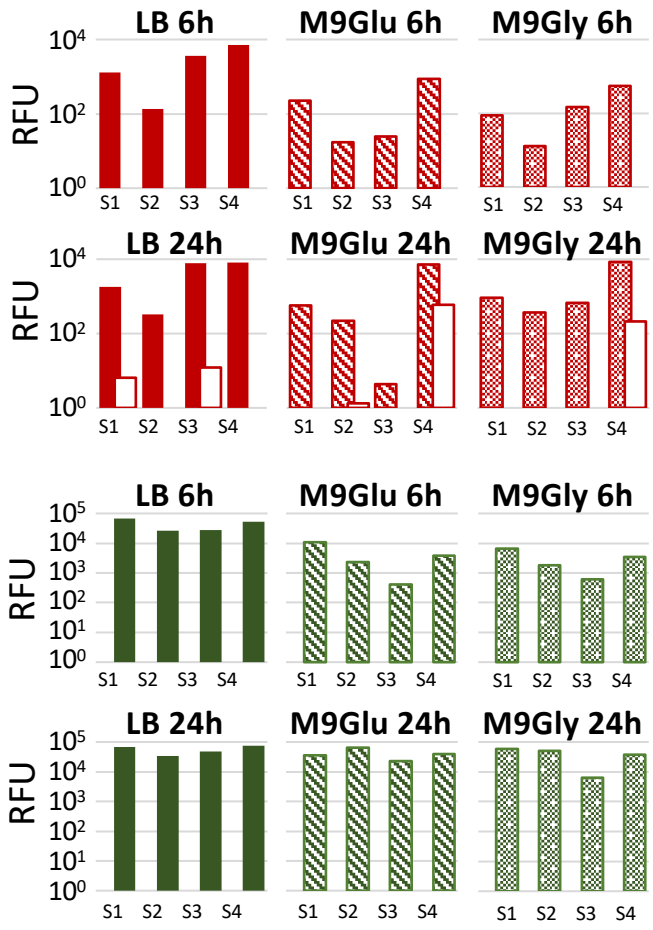

Supplementary Figure 5: Independent expression from strains with two plasmids in the presence of a single inducer. Toolbox plasmids were induced with the mRFP cognate inducer (top, red) or the GFP cognate inducer (bottom, green). Expression from the cognate inducer (solid and patterned bars) and expression from the non-cognate inducer (open bars). RFU data in is background and basal expression-subtracted. All data is the average of triplicates. Details in Supplementary Note 1.

Supplementary Note 1: Independent induction of two-plasmid systems.

The induction of each toolbox system independently showed that only one promoter-regulator pair had a strong response with the non-cognate inducer (Supplementary Figure 5). While expression was maintained under 3-fold from the uninduced reporter in mS1, mS2, and mS3, there was notable mRFP expression from $VanR^{AM}/P_{VanCC}$ in mS4 by stationary phase in the presence of the Lux inducer OC6. Here, mRFP induced by the non-cognate inducer expressed 80-fold over basal levels in M9Glu and 2-fold over basal expression in M9Gly, where leaky expression was very high by the 24h timepoint. When induced with only vanillate, $VanR^{AM}$-regulated expression of mRFP in mS4 had the highest expression at late-exponential phase of all strains tested across culturing media, but high levels of basal expression reduced fold change by over 75% after overnight growth in LB and M9Gly. This is consistent with data from the $VanR^{AM}$-regulated system across different backbones in single plasmid experiments in *E. coli* MG1655 (Figure 1D-E).

Independent expression after an overnight induction showed that the strain with the highest expression is inconsistent across media types (Supplementary Figure 5). While pEVR4 in mS4 has the highest overall induced expression of mRFP in both rich and minimal media, results are less consistent in different culturing conditions for GFP and the leakiness varies widely for both reporters. For example, the $LuxR/P_{LuxB}$ system in mS3 expresses mRFP over 320-fold after an overnight induction in LB but the fold change is 16 and 0 in M9Gly and M9Glu, respectively, due to leaky expression. Inconsistencies in leaky expression and overall inducibility across media types highlight the effect of host metabolism on the behavior of different inducible systems.

Similarly, expression levels from strains grown in minimal media supplemented with the two different carbon sources are not consistently higher in one over another. In general, mRFP-expressing plasmids had higher outputs when glycerol was used as the sole carbon source. Otherwise, induction profiles in M9Glu and M9Gly generally follow the same trends, with the exception of $VanR^{AM}$-regulated expression of mRFP in M9Glu as mentioned above.

mS1, mS2, and mS3 possess the $CymR^{AM}/P_{CymRC}$ and $LuxR/P_{LuxB}$ promoter-regulator pairs on different plasmid backbones. The same plasmid pELxG4 is present in both mS1 and mS2, providing a direct comparison of the effect of the second plasmid in each two-plasmid system. While our data suggests that the promoter-regulator has the largest effect on expression, plasmid copy number is also known to affect expression (12). Though the pCDFDuet-1 plasmid has a similar copy number to the pCOLADuet-1 plasmid, our data shows that pCCyR2 has higher overall expression at both late-exponential phase and stationary phase in all media types compared to pDCyR1, with fold change values over 15 times higher at both timepoints (Figure 1D-E).

We next compared expression amongst the toolbox plasmids, where strains mS1, mS2, and mS3 all possessed both Cy and Lx regulators, but differed by origin and marker (Figure 5). By stationary phase, independent expression of mRFP from pCCyR2 (mS1) and pDCyR1 (mS2) in LB was between 60 and 70-fold (Supplementary Figure 5), but interestingly mS2 expresses 2-fold higher in the presence of both OC6 and cumate compared to mS1 under the same conditions. These trends are echoed in the minimal media with mS2 exhibiting the highest fold change in mRFP expression of the four strains in the presence of both inducers. mS3 contains the same $CymR^{AM}/P_{CymRC}$ and $LuxR/P_{LuxB}$ systems and here, pDLxR6 has the highest expression of mRFP in LB by stationary phase, both in the presence of only OC6 and in the presence of OC6

and cumate. Conversely, pACyG1 has the lowest expression of GFP in the presence of both inducers of all four toolbox strains in rich media, possibly due to the metabolic burden of the simultaneously induced LuxR/P_{LuxB} system. Surprisingly, LuxR-regulated mRFP expression in mS3 at stationary phase was below 20-fold in M9Glu and M9Gly, partially due to a high level of leaky expression. Expression from pACyG1 in mS3 was not above background in the presence of both cumate and OC6, but when induced independently, expression was 91- and 23-fold in M9Glu and M9Gly respectively (Supplementary Figure 5). These induction profiles exemplify how changing plasmid pairings and culturing media influences independent and dual expression in multi-plasmid systems in unexpected ways.

Supplementary References

1. Choi,Y.J., Morel,L., François,T. Le, Bourque,D., Lucie,B., Groleau,D., Massie,B. and Miguez,C.B. (2010) Novel, versatile, and tightly regulated expression system for Escherichia coli strains. *Appl. Environ. Microbiol.*, **76**, 5058–5066.
https://doi.org/10.1128/AEM.00413-10

2. Stanton,B.C., Nielsen,A.A.K., Tamsir,A., Clancy,K., Peterson,T. and Voigt,C.A. (2014) Genomic mining of prokaryotic repressors for orthogonal logic gates. *Nat. Chem. Biol.*, **10**, 99–105.
https://doi.org/10.1038/nchembio.1411

3. Meyer,A.J., Segall-Shapiro,T.H., Glassey,E., Zhang,J. and Voigt,C.A. (2019) Escherichia coli "Marionette" strains with 12 highly optimized small-molecule sensors. *Nat. Chem. Biol.*, **15**, 196–204.
https://doi.org/10.1038/s41589-018-0168-3

4. Moon,T.S., Lou,C., Tamsir,A., Stanton,B.C. and Voigt,C.A. (2012) Genetic programs constructed from layered logic gates in single cells. *Nature*, **491**, 249–253.
https://doi.org/10.1038/nature11516
http://www.ncbi.nlm.nih.gov/pubmed/23041931

5. Kaczmarczyk,A., Vorholt,J.A. and Francez-Charlot,A. (2014) Synthetic vanillate-regulated promoter for graded gene expression in Sphingomonas. *Sci. Rep.*, **4**, 4–7.
https://doi.org/10.1038/srep06453

6. Kunjapur,A.M. and Prather,K.L.J. (2019) Development of a Vanillate Biosensor for the Vanillin Biosynthesis Pathway in E. coli. *ACS Synth. Biol.*, **8**, 1958–1967.
https://doi.org/10.1021/acssynbio.9b00071
http://www.ncbi.nlm.nih.gov/pubmed/31461264

7. Held,D., Yaeger,K. and Novy,R. (2003) New coexpression vectors for expanded compatibilities in E. coli. *Innovations*.

8. Schuster,L.A. and Reisch,C.R. (2021) A plasmid toolbox for controlled gene expression across the Proteobacteria. *Nucleic Acids Res.*, **49**, 7189–7202.
https://doi.org/https://doi.org/10.1093/nar/gkab496

9. Zhang,J.J., Tang,X., Zhang,M., Nguyen,D. and Moore,B.S. (2017) Broad-host-range expression reveals native and host regulatory elements that influence heterologous antibiotic production in Gram-negative bacteria. *MBio*, **8**, e01291-17.
https://doi.org/10.1128/mBio.01291-17
http://www.ncbi.nlm.nih.gov/pubmed/28874475

10. Chatzivasileiou,A.O., Ward,V., Edgar,S.M. and Stephanopoulos,G. (2019) Two-step pathway for isoprenoid synthesis. *Proc. Natl. Acad. Sci. U. S. A.*, **116**, 506–511.

https://doi.org/10.1073/pnas.1812935116
http://www.ncbi.nlm.nih.gov/pubmed/30584096

11. Kovach,M.E., Elzer,P.H., Hill,D.S., Robertson,G.T., Farris,M.A., Roop,R.M. and Peterson,K.M. (1995) Four new derivatives of the broad-host-range cloning vector pBBR1MCS, carrying different antibiotic-resistance cassettes. *Gene*, **166**, 175–176.

12. Brewster,R.C., Weinert,F.M., Garcia,H.G., Song,D., Rydenfelt,M. and Phillips,R. (2014) The transcription factor titration effect dictates level of gene expression. *Cell*, **156**, 1312–1323.
https://doi.org/10.1016/j.cell.2014.02.022